nature
biotechnology

Characterization of voltage-gated sodium-channel blockers by electrical stimulation and fluorescence detection of membrane potential

Chien-Jung Huang, Alec Harootunian, Michael P Maher, Catherine Quan, Christopher D Raj, Ken McCormack, Randal Numann, Paul A Negulescu & Jesús E González

Voltage-gated ion channels regulate many physiological functions and are targets for a number of drugs. Patch-clamp electrophysiology is the standard method for measuring channel activity because it fulfils the requirements for voltage control, repetitive stimulation and high temporal resolution, but it is laborious and costly. Here we report an electro-optical technology and automated instrument, called the electrical stimulation voltage ion probe reader (E-VIPR), that measures the activity of voltage-gated ion channels using extracellular electrical field stimulation and voltage-sensitive fluorescent probes. We demonstrate that E-VIPR can sensitively detect drug potency and mechanism of block on the neuronal human type III voltage-gated sodium channel expressed in human embryonic kidney cells. Results are compared with voltage-clamp and show that E-VIPR provides sensitive and information-rich compound blocking activity. Furthermore, we screened ~400 drugs and observed sodium channel–blocking activity for ~25% of them, including the antidepressants sertraline (Zoloft) and paroxetine (Paxil).

Voltage-gated sodium (Na_v) channels generate rapid, transient inward currents that drive the upstroke of the action potential of excitable cells such as neurons and striated muscle. Na_v channels are also the target of many drugs, including anesthetics, analgesics, antiepileptics and antiarrhythmics[1–3]. A common property of these drugs is that they preferentially affect the channel at a specific stage of its cycle of rest, activation and inactivation, often by delaying the recovery from the inactivated state, thereby producing a cumulative reduction of Na^+ currents[4]. This 'use-dependent' block allows these drugs to preferentially act on cells and nerves firing at different frequencies and is important for the therapeutic index[5], as known agents demonstrate little or no selectivity for Na_v-channel subtypes[6]. The whole-cell voltage clamp is an elegant and useful method to study such properties because it offers sufficient voltage control and temporal resolution to track the millisecond kinetics of activation and inactivation. Unfortunately, conventional electrophysiological methods have extremely low throughput, limiting the number of channels and agents that can be conveniently studied. Recently introduced planar patch techniques are more efficient than traditional electrophysiology[7], but these approaches still have cost, throughput and technical constraints that limit large-scale screening and profiling of ion channels[8]. Nonelectrophysiological high-throughput screening techniques, including the application of voltage-sensitive dyes[9–11], have also been developed to facilitate ion-channel drug discovery. Although robust and cost effective, these screening approaches are not well suited to study state dependence because they use nonphysiological stimulation methods such as pharmacological modifiers[12], cannot repetitively stimulate the channel and have low temporal resolution.

To combine the convenience and throughput of screening methods with some of the stimulation control and temporal resolution afforded by electrophysiology, we have developed E-VIPR, an electro-optical approach that combines variable, repetitive electrical field stimulation (EFS) and detection of membrane potential by voltage-sensitive dyes to stimulate and record channel activity[13,14]. The approach provides an extracellular electrode array to cells in standard 96- and 384-well microtiter plates to achieve higher throughput, greater reliability and lower cost than either electrophysiology or commercially available planar patch systems. We compared E-VIPR results with electrophysiology by testing known Na_v-channel blockers in cells expressing the human type III voltage-gated sodium channel ($hNa_v1.3$), and found a high correlation between the two techniques for determining both potency and use-dependence of compounds. $hNa_v1.3$ is an attractive drug target for treating pain because it is upregulated after nerve injury[15] and in inflammatory pain models[16]. To demonstrate the utility of this technology for rapidly characterizing compounds, we profiled ~400 clinically used drugs and found that antidepressants with diverse chemical structures inhibit Na_v channels, a previously unreported feature that may contribute to the effects of these drugs in humans. We conclude that the E-VIPR offers a convenient platform to support large-scale research and drug discovery for voltage-gated ion-channel targets.

Vertex Pharmaceuticals Incorporated, 11010 Torreyana Road, San Diego, California 92121, USA. Correspondence should be addressed to J.E.G. (Tito_Gonzalez@sd.vrtx.com).

Received 8 August 2005; accepted 5 January 2006; published online 19 March 2006; corrected 27 March 2006 (details online); doi:10.1038/nbt1194

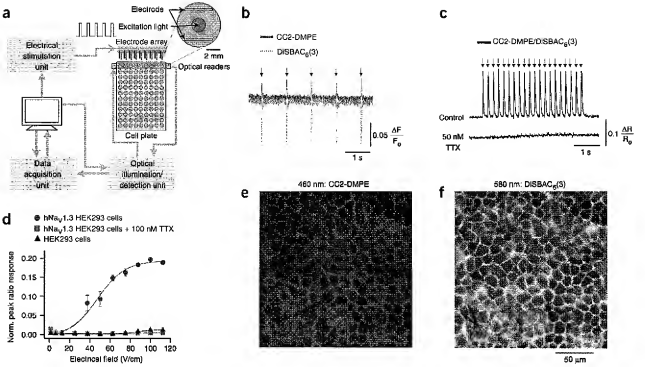

Figure 1 Measurements of Na_v channel–dependent voltage changes with E-V/PR. (**a**) Scheme of E-V/PR instrumentation. Cells cultured in a 96-well microtiter plate are simultaneously stimulated with eight parallel electrode pairs that dip into each well. Monophasic stimulation voltage pulses are created with a function generator, which are converted to currents with a voltage-to-current amplifier and delivered to the electrodes. Light from a xenon arc lamp is passed through 400-nm interference filters, to select the excitation wavelength. Both excitation and emission light are directed to and from the bottom of the plate by eight trifurcated optical fiber bundles. One leg of the trifurcated fiber is used as an excitation source and the other two are used to detect fluorescence emission at 460 and 580 nm, for CC2-DMPE and $DiSBAC_6(3)$ respectively. An enlargement of a single well diagrams the electrode orientation and optical field of view. Fluorescence emission is detected with photomultipliers before, during and after electrical stimulation. (**b**) Electrical field stimulation elicits membrane-potential transients detected by voltage-sensitive FRET probes. Individual normalized fluorescence signals from CC2-DMPE (blue trace) and $DiSBAC_6(3)$ (red trace) were measured from HEK293 cells expressing $hNa_v1.3$ during 1-Hz EFS train of voltage steps from 0 to 100 V/cm. Arrows indicate when stimulation was applied. Ratiometric FRET responses are indicative of repetitive transient depolarizations, which are synchronous with electrical stimulation. (**c**) TTX blocks $hNa_v1.3$–dependent FRET signals. The normalized CC2-DMPE over $DiSBAC_6(3)$ FRET ratio signal, black trace, indicates the membrane-potential response to 5 Hz train of voltage steps from 0 to 100 V/cm (top). Arrows indicate when the stimulation was applied. 50 nM TTX completely blocks the stimulated depolarizations (bottom) demonstrating that it is dependent on the TTX-sensitive $hNa_v1.3$. (**d**) Stimulation strength versus membrane-potential response. Normalized peak ratio responses to a 5 Hz train of voltage pulses are plotted as a function of electrical field strength (1–113 V/cm) in the absence (blue circles) and presence (red squares) of 100 nM TTX. EFS-induced depolarizations are blocked by TTX at all field strengths tested indicating that they are due to $hNa_v1.3$ activation and not nonspecific electroporation. No membrane depolarizations were observed in cells not transfected with $hNa_v1.3$ (black triangles). Data are shown as mean ± s.e.m. ($n = 4$). (**e**,**f**) Fluorescence images of live HEK293 cells stained with CC2-DMPE and $DiSBAC_6(3)$. Cells were excited at 400 nm and the CC2-DMPE and $DiSBAC_6(3)$ emission was observed with a fluorescent microscope at 460 (**e**) and 580 (**f**) nm, respectively.

RESULTS

E-VIPR stimulates and detects Na_v-channel activity

The E-VIPR screening system consists of a computer-controlled electrode array integrated with an 8-channel dual-emission wavelength fluorescence reader (**Fig. 1a**). Membrane potential was monitored using the high-speed voltage-sensitive probe combination of CC2-DMPE and DiSBAC6(3), which undergo fluorescence resonance energy transfer (FRET) based on the potential[17,18]. Representative fluorescence signals obtained from human embryonic kidney (HEK)293 cells expressing $hNa_v1.3$ in response to five 2-ms monophasic EFS pulses delivered at 1 Hz are shown (**Fig. 1b**). The fluorescence ratio change ΔR was used to measure 5-Hz EFS-induced membrane-potential changes (**Fig. 1c**). The response was blocked by 50 nM tetrodotoxin (TTX) and was absent in untransfected HEK293 cells, showing that the membrane-potential changes were due to activation of $Na_v1.3$, which are tetrodotoxin (TTX) sensitive (**Fig. 1d**). The cells have a resting membrane potential of approximately −65 mV, and the transient response consists of a depolarization due to the opening of Na_v channels followed by a repolarization due to sodium channel inactivation, the activity of endogenous K^+ channels and the rectification properties of the membrane. The membrane potential as a function of stimulation strength (**Fig. 1d**) shows that peak response increases with field strength, consistent with activation of additional channels as the field strength increases. Fields >25 V/cm evoked TTX-sensitive, $hNa_v1.3$–dependent depolarizations with no evidence of electroporation up to 113 V/cm, the greatest field strength tested. Electroporation was assessed as an irreversible depolarization that could not be blocked by TTX. This type of response has been observed with some EFS protocols that have greater stimulation strengths and/or duty cycles (not shown). Because a field strength of 100 V/cm produced the largest and fastest E-VIPR response with no evidence of cell damage, this field strength was used in most

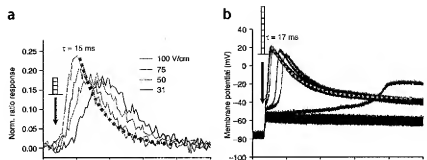

Figure 2 E-VIPR signals and membrane-potential changes. **(a)** Magnitude and kinetics of E-VIPR recordings. Millisecond time resolution FRET membrane-potential response to increasing EFS strength. Normalized FRET ratio responses were elicited from $hNa_v1.3$-expressing cells applying voltage pulses with amplitudes ranging from 31 to 100 V/cm. The magnitude and speed of depolarization increased with increasing stimulation field strength, with largest 100 V/cm producing ~25% ratio change with a rise time <10 ms. **(b)** Magnitude and kinetics of current-clamp recordings. Membrane-potential responses were also elicited by intracellular current injection. Whole-cell current-clamp data were obtained from a cell in monolayer using a series of 1-ms depolarizing current steps from 500–850 pA in 50-pA increments. Similar membrane-potential response properties including increasing rate of depolarization, amplitude, time to maximum voltage change and relaxation time constants are observed for both methods. Exponential fits of the repolarization, with maximal stimulation, are plotted for both methods (dotted lines) and gave similar time constants of ~15 ms.

subsequent experiments. Fluorescence images of $hNa_v1.3$-expressing cells in plates are shown using band-pass emission filters for CC2-DMPE (**Fig. 1e**) and $DiSBAC_6(3)$ (**Fig. 1f**) and demonstrate that the fluorescence is restricted to the plasma membrane.

Characterization of E-VIPR-induced membrane-potential changes

We compared the magnitude, sensitivity and kinetics of EFS-induced FRET ratio signals (**Fig. 2a**) with current-clamp electrophysiology (**Fig. 2b**). Both techniques produced a regenerative membrane-potential response once an activation threshold was reached, consistent with activation of Na_v channels. Both the rate and magnitude of the FRET response increased with increasing EFS strength. A field strength of 100 V/cm produced an ~25% FRET ratio increase. Previous work has shown that the FRET response is approximately linear between –80 and +40 mV[17,19], with a sensitivity of ~10–60% $\Delta R/R$ per 100 mV[17,18], depending on experimental conditions. We used high K^+ depolarization in E-VIPR to determine a sensitivity of ~20%/100 mV (not shown) and estimate that EFS-induced responses correspond to depolarizations of ~100 mV. Because E-VIPR can reliably detect ratio changes of ~3%, we estimate that the optical method can reliably detect membrane-potential changes as small as 15 mV. Using current injection, we elicited depolarizations up to 100 mV above threshold (**Fig. 2b**) and compared the time courses of the responses. The time courses for depolarization (<10 ms) and

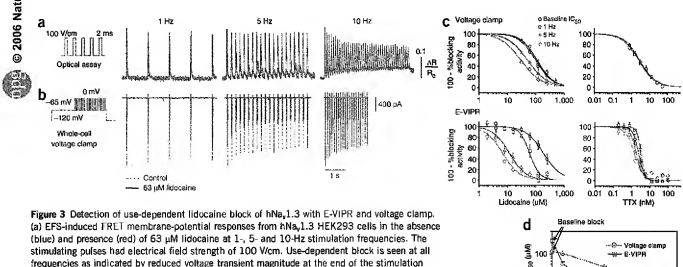

Figure 3 Detection of use-dependent lidocaine block of $hNa_v1.3$ with E-VIPR and voltage clamp. **(a)** EFS-induced FRET membrane-potential responses from $hNa_v1.3$ HEK293 cells in the absence (blue) and presence (red) of 63 μM lidocaine at 1-, 5- and 10-Hz stimulation frequencies. The stimulating pulses had electrical field strength of 100 V/cm. Use-dependent block is seen at all frequencies as indicated by reduced voltage transient magnitude at the end of the stimulation train compared to the first peak and drug-free traces. **(b)** The analogous whole-cell voltage-clamp experiment shows use-dependent lidocaine block of inward Na^+ currents. The cells were held at –120 mV, followed by a 1.5-s conditioning pulse to –65 mV, and then 20-ms pulse trains to 0 mV were applied at 1, 5 and 10 Hz. Schematics of the assay protocols are shown to the left of the traces. **(c)** Voltage-clamp (top) and E-VIPR (bottom) concentration-response curves are plotted for lidocaine and TTX. Baseline and use-dependent block were determined from the amplitude of either current or FRET ratio response to the first (P1) and 20th (P20) stimulation pulses, respectively. In both assays, the lidocaine curves show large shifts to lower concentrations with increased stimulation compared to TTX. For both molecules greater potency shifts were observed on E-VIPR **(d)** Lidocaine IC_{50}s for baseline and each frequency are plotted for each method. Both methods show general agreement in that relatively little block is observed on the first stimulation pulse and that the degree of block increases as the stimulation frequency increases. The frequency dependence of block is steeper and detected more sensitively on E-VIPR.

Table 1 Comparison of IC_{50} (mean ± s.e.m.)

	Baseline		1 Hz		5 Hz		10 Hz	
	V-clamp	E-VIPR	V-clamp	E-VIPR	V-clamp	E-VIPR	V-clamp	E-VIPR
TTX (nM)	2.8 ± 0.1	2.5 ± 0.1	2.5 ± 0.2	3.4 ± 0.1	2.9 ± 0.2	1.9 ± 0.1	2.6 ± 0.2	1.5 ± 0.2
Tetracaine (μM)	1.7 ± 0.1	3.7 ± 0.3	0.9 ± 0.0	0.8 ± 0.1	0.7 ± 0.0	0.4 ± 0.0	0.8 ± 0.1	0.3 ± 0.0
Riluzole (μM)	0.3 ± 0.0	7.8 ± 0.4	ND	ND	ND	ND	0.2 ± 0.0	0.5 ± 0.0
Amitriptyline (μM)	3.5 ± 0.2	5.0 ± 0.2	1.5 ± 0.1	2.1 ± 0.2	1.3 ± 0.1	1.4 ± 0.7	1.4 ± 0.1	1.2 ± 0.1
Etidocaine (μM)	8.1 ± 0.7	28.0 ± 1.8	ND	ND	ND	ND	2.4 ± 0.5	1.2 ± 0.0
Mexiletine (μM)	74.8 ± 3.4	30.6 ± 1.8	55.4 ± 3.0	23.1 ± 2.2	34.8 ± 1.4	7.8 ± 1.0	27.4 ± 1.2	3.3 ± 0.2
Lidocaine (μM)	113.6 ± 8.2	188.1 ± 13.8	101.7 ± 1.8	61.8 ± 5.7	52.0 ± 1.5	11.7 ± 1.5	30.4 ± 2.2	6.8 ± 1.0
Lamotrigine (μM)	102.2 ± 2.2	118.7 ± 6.9	84.2 ± 6.2	42.3 ± 4.1	68.3 ± 3.7	17.8 ± 0.9	51.0 ± 3.3	8.9 ± 0.9
Carbamazepine (μM)	352.0 ± 12.9	168.0 ± 4.6	ND	ND	ND	ND	163 ± 16.4	19.0 ± 2.4

ND, not determined.

repolarization (time constant $\tau \sim 15$ ms) are similar for both methods, indicating that the optical method accurately tracks membrane potential.

Detection of different blocking mechanisms

We evaluated the ability of the E-VIPR technique to distinguish between use-dependent and non-use-dependent (baseline) block of $hNa_v1.3$ using lidocaine and TTX, respectively. Lidocaine is a widely used local anesthetic whose mechanism of action is use-dependent block of Na_v channels[20] and which has been shown to block different Na_v-channel subtypes, including $hNa_v1.3$ (ref. 21), with approximately equal potency. TTX is a potent blocker with very weak voltage- and use-dependence that binds to a different site from lidocaine[22]. **Figure 3a,b** shows the blocking properties of 63 μM lidocaine on $hNa_v1.3$ in both voltage-clamp recording and E-VIPR, when stimulating at **1**, 5 and 10 Hz. The lidocaine block reduced the voltage response upon repetitive stimulation at each frequency compared to control without drug. In both formats, the peak ratio responses to the first and the 20th EPS pulse, denoted as **P1 and P20, were** normalized to the response without drug to assess the **degree of baseline** and use-dependent block, respectively, for each frequency. **Figure 3c** shows lidocaine and TTX concentration–response plots for both baseline and use-dependent block at 1, 5 and 10 Hz using voltage clamp and E-VIPR. The lidocaine baseline-block IC_{50} values were similar at 110 and 190 μM, respectively. Upon repetitive 10-Hz stimulation, blocking potencies increased to 30 and 7 μM by voltage clamp and E-VIPR, respectively. Thus, despite the technique differences, both methods report more potent block at higher stimulation frequencies, as expected for a use-dependent blocker. However, E-VIPR did show a steeper dependence of block potency on stimulation frequency (Fig. 3d).

In contrast, the IC_{50} for TTX was essentially independent of stimulation frequency, and block was similar on P1 and P20 (Fig. 3c). A relatively small potency increase at higher frequencies was observed for TTX in the E-VIPR assay, which is consistent with reports of modest TTX use-dependence[23,24].

Potency and use-dependence ranking of drugs

To further characterize the molecular pharmacology results obtained with E-VIPR, we determined the concentration-response curves for inhibition of $hNa_v1.3$ by eight well-characterized drugs that cause use-dependent block of Na_v channels: tetracaine[25], riluzole (Rilutek)[26], amitriptyline[27–29], etidocaine (Duranest)[30], mexiletine (Mexitil)[31], lidocaine[21], lamotrigine (Lamictal)[32–34] and carbamazepine (Tegretol)[33]. In addition, we studied TTX. Only lidocaine has been previously tested against $hNa_v1.3$, although these drugs generally block the different subtypes with approximately equal affinities. E-VIPR and voltage-clamp concentration-response curves were determined for

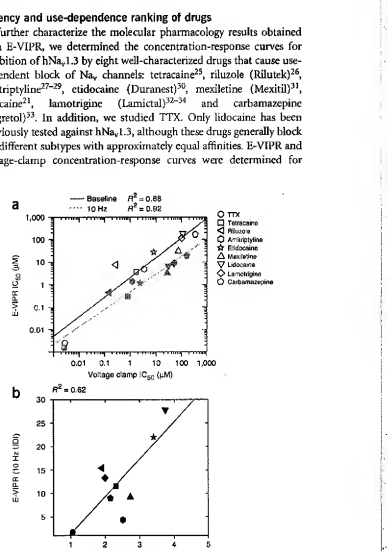

Figure 4 Blocking properties of Na_v-channel drugs in E-VIPR and voltage clamp. A comparison of the $hNa_v1.3$-blocking potencies and use-dependent activities of the nine blockers listed in **Table 1**: TTX, tetracaine, riluzole, amitriptyline, etidocaine, mexiletine, lidocaine, lamotrigine and carbamazepine are presented. (a) E-VIPR baseline (blue) and 10-Hz (red) blocking IC_{50} values are plotted versus those obtained with voltage clamp. Linear fits to the data are drawn and show a high correlation with R^2 values of 0.88 and 0.92 for baseline (blue) and 10 Hz (red) use-dependent block, respectively. The compounds, to varying degrees, block with greater potencies at 10 Hz. This is seen in the E-VIPR data as the red 10-Hz data are shifted downward to more potent IC_{50}s from the blue baseline data. (b) Correlation of use-dependent block index measurements between E-VIPR and voltage clamp are plotted.

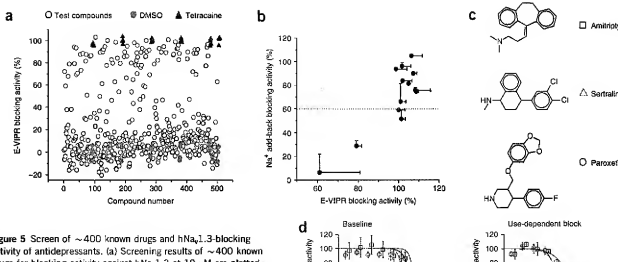

Figure 5 Screen of ~400 known drugs and hNa$_V$1.3-blocking activity of antidepressants. (**a**) Screening results of ~400 known drugs for blocking activity against hNa$_V$1.3 at 10 μM are plotted. Data were obtained from hNa$_V$1.3-expressing cells using the 5-Hz stimulation protocol described in **Figure 3a**. Each plate contained four negative (DMSO, red circles) and four positive (100 μM tetracaine, blue triangles) control wells. The average screening window was excellent with $Z' = 0.71$. Drug-blocking activity was calculated from the controls and hits were defined as >60% of the tetracaine block. (**b**) Antidepressants from different chemical series were enriched (13/18) in hNa$_V$1.3-blocking activity relative to other drug classes. These identified blockers were used to compare E-VIPR with a VIPR membrane-potential assay that uses Na^+ exchange and the pharmacological modifiers veratridine and deltamethrin. The blocking activities are plotted for the two assays and demonstrate that E-VIPR more sensitively detects the active antidepressants, including mirtazapine and bupropion, that were missed in the VIPR assay (below horizontal line). (**c**) The structures of amitriptyline, sertraline and paroxetine are shown. (**d**) E-VIPR concentration-response relationships of these antidepressants for baseline (left) and use-dependent block (right) are shown. These antidepressants show use dependent block with UDIs > 1.5.

baseline and use-dependent block at 1, 5 and 10 Hz, and the IC_{50} values are given (**Table 1**). For all compounds except TTX, we found an intermediate drug concentration at which the block greatly increased during the stimulation train from P1 to P20, indicating the expected use-dependent block. To compare baseline and use-dependent blocking potencies of the two approaches for different blockers, we plotted the E-VIPR and voltage-clamp baseline and 10-Hz IC_{50} values (**Fig. 4a**). A linear fit of the data indicate a high correlation ($R^2 = 0.9$) between both measures, with E-VIPR being consistently more sensitive at 10 Hz. Riluzole is an outlier because of a very potent baseline block using the voltage clamp, which suggests that riluzole is able to access its high-affinity site[35] with this protocol.

To compare the relative use-dependence of Na$_V$-channel blockers, we calculated the ratio of baseline or tonic IC_{50} to use-dependent IC_{50} for each compound, a value that we have termed the use-dependent index (UDI; **Fig. 4b**). A linear fit of data gave a correlation with $R^2 = 0.62$. In all cases the UDIs were lower when measured by voltage clamp, with the use-dependent block being more potent in E-VIPR. Both methods accurately assign compounds into low (TTX), medium and high (lidocaine and etidocaine) use-dependent activity categories. Overall, these data demonstrate that the E-VIPR assay can accurately distinguish between compounds with different potencies and degrees of use-dependence.

Enriched Na$_V$-channel blocking activity in drugs

We applied the E-VIPR membrane-potential assay to screen ~400 drugs for hNa$_V$1.3-blocking activity at 10 μM in 96-well microtiter plates (**Fig. 5a**). An excellent Z′ screening window[36] of 0.71 ± 0.11 between the the positive (100 μM tetracaine) and negative (0.1% DMSO) controls was attained, which is compatible with high-throughput screening. Interestingly, ~25% of the drugs had use-dependent blocking activity that was >60% of that of tetracaine controls. The high hit rate was approximately double the rate found screening diverse commercial small molecule libraries against hNa$_V$1.3 (data not shown), suggesting that Na$_V$-channel activity is enriched in drugs. In particular, antidepressants were highly enriched, with 13 out of 18 compounds active in the screen. The antidepressants identified in the screen are desipramine, protriptyline, paroxetine, sertraline, trimipramine, amitriptyline, fluoxetine (Prozac), fluvoxamine, doxepin, sibutramine, nefazodone (Serzone), mirtazapine and bupropion (Wellbutrin). All blocked hNa$_V$1.3 completely, except mirtazapine (79%) and bupropion (61%).

To compare E-VIPR with a conventional membrane-potential assay, we screened the identified Na$_V$ channel–blocking antidepressants with a Na^+ add-back VIPR assay[19] that uses extracellular Na^+ exchange and veratridine plus deltamethrin to keep the channel open (**Fig. 5b**). The E-VIPR assay more sensitively detected active compounds and identified fluvoxamine, mirtazapine and bupropion, which were missed in the VIPR assay using a hit cut off of 60% tetracaine activity. The Na$_V$ channel-blocking activity of these antidepressants, except for amitriptyline, desipramine, fluoxetine and doxepin, have not, to our knowledge, been previously reported. Detailed concentration responses are shown in **Figure 5**, and these potencies were confirmed with voltage-clamp studies (data not shown). In addition, the drugs were found to block human Na$_V$1.2, Na$_V$1.5, Na$_V$1.7, and Na$_V$1.8 with similar potencies to Na$_V$1.3 with E-VIPR.

DISCUSSION

Electrical field stimulation has been used to manipulate and study excitable biological systems ever since Galvani and Volta discovered around 1790 that electrical stimulation elicits muscle contractions in frogs[37], and it has been used to activate individual nerves, neurons and cardiac cells[38,39]. In addition, electrical stimulation has been used to treat neurological conditions such as pain[40]. Recently, a related approach has been reported that used stimulating electrodes fabricated on transparent surfaces together with slow-responding (tens of seconds) fluorescent probes of membrane potential to detect endogenous sodium-channel activity in neuroblastoma cells[41].

E-VIPR combines EFS and detection of membrane potential using high-speed FRET membrane-potential dyes to enable sensitive high-throughput assays of voltage-gated ion channels. It provides high throughput and screening reliability similar to that seen with established microtiter plate–based VIPR[19] and fluorescence imaging plate reader systems[42]. However, the information content is more like that obtained from current-clamp electrophysiology in that a variable, repetitive, electrical stimulation is used to activate the channels and the membrane potential is allowed to change in response to ion fluxes across the cell membrane. EFS duration and FRET voltage sensor dye temporal response are well matched at ~2 ms and together are sufficient to measure the peak of channel-dependent transient depolarizations, which have a rise time <10 ms (**Fig. 2**). We demonstrate the utility of the technology using $hNa_V1.3$, a potential target for neuropathic pain. Na_V channels represent a particularly relevant target class for E-VIPR assays because of their rapid gating kinetics, voltage dependence, low cellular expression and the state dependence of many blockers.

This approach has several attractive features that distinguish it from voltage clamp and other ion-channel assay methods. First, a pharmacological block can be assessed in cells expressing very few channels without dialysis of intracellular components. Na_V-channel assays require a high sensitivity to ion flux as the channels are open only for milliseconds. High sensitivity is achieved because large membrane-potential changes (tens of mVs) result from a small number of ions (10^6) passing across the high-resistance membrane. Consistent with this property, we have observed large voltage-sensitive FRET changes in cell lines that have current densities as low as 3–5 pA/pF (data not shown). This is important because some channels, such as $hNa_V1.8$ (ref. 25) and $hNa_V1.9$ (ref. 43), are difficult to express heterologously in standard Chinese hamster ovary and HEK293 screening cell lines.

Second, the time course of a slowly developing block can be assessed, which is challenging with patch clamp because it requires maintaining a stable high-resistance seal for long time periods. Slow-acting compounds are likely to be missed with voltage-clamp screens, which typically have compound exposures ≤5 min because of technical and throughput limitations. A third advantage over standard fluorescence assays is that Na_V channels are not modified by 'agonists.' Previous high-throughput optical methods required channel openers, such as veratridine, deltamethrin or batrachatoxin, to tonically activate the channels[12,19,44,45], which compromises the detection of a state-dependent block. A direct comparison of E-VIPR to a VIPR membrane-potential assay that required extracellular Na^+ exchange and veratridine/deltamethrin demonstrated that E-VIPR detected Na_V-channel blockers more sensitively, including drugs that were missed by VIPR, based on screening a panel of antidepressants (**Fig. 5b**). A more extensive screening comparison and analysis will be required to fully characterize the different types of blockers detected by the two optical methods.

Finally, the assay is inexpensive and high-throughput and therefore allows broad screening and profiling of compounds and targets. For example, factoring in both time and reagents, an E-VIPR data point costs ~$0.03, 100 times lower than the cost of a planar patch data point (based primarily on consumable costs)[8], and takes about 1,000-fold less time than our estimate of a conventional manual patch-clamp recording based on the estimated throughput of one compound profiled per electrophysiologist per day.

We found that E-VIPR accurately detects the potency and use-dependence of Na_V-channel block based on a comparison to voltage-clamp results. We analyzed the data by measuring changes in the magnitude of depolarization, though other methods could also be envisioned, such as measuring changes in rates of depolarization. At high stimulation frequencies E-VIPR generally detected a block with approximately fivefold higher sensitivity compared with voltage clamp (**Fig. 4a**). The increased sensitivity could be the result of several factors, including different assay holding potentials or the threshold nature of the voltage response, which might require less channel block to inhibit the depolarization. The increased detection sensitivity is most evident with prolonged stimulation and may be due to differences in cellular membrane potentials or intrinsic susceptibility to block at the end of a stimulation train. Both baseline and use-dependent E-VIPR IC_{50} values were found to correlate very well ($R^2 = 0.9$) with analogous voltage-clamp determinations. We used the ratio of baseline to use-dependent IC_{50}s as a measure of use-dependence (UDI) that includes both voltage and frequency components of block. E-VIPR UDIs also correlated with those from voltage-clamp recordings ($R^2 = 0.62$), but to a lesser degree (**Fig. 4b**). Analysis of the outliers riluzole and amitriptyline suggested that, unlike most of the drugs profiled, these compounds have baseline or tonic IC_{50} values that include substantial activity contributions from the high-affinity inactivated state, based on comparisons to published values[27,35]. The disparate use-dependence sensitivity likely reflects mechanistic differences that are differentially sensed by the two techniques; additional work is needed to fully understand the relationship between use-dependence and the measurement technique.

Whereas E-VIPR generally correlates well with the patch-clamp technique and certain aspects of E-VIPR are analogous to patch clamp, E-VIPR cannot clamp the membrane potential and is not intended as a replacement for this important technique. The limited voltage control of E-VIPR constrains the range of stimulation and voltage protocols possible for measuring channel and compound activity. For example, cell lines with different resting membrane potentials have different percentages of channels in resting and inactivated states, which can influence their sensitivities to compound block. Assay development for E-VIPR must take such factors into account to accurately compare compound block in cell lines expressing different channel subtypes. Voltage-clamp electrophysiology is complementary to E-VIPR and we see its use to support final biophysical characterization of a limited number of compounds, when throughput and cost are no longer limiting to drug discovery.

The E-VIPR screen against $hNa_V1.3$ of clinically used drugs showed that a surprisingly large percentage (~25%) of the tested drugs have Na_V channel–blocking properties. Of the different drug classes, antidepressants showed the most unexpected and striking overlap: 72% of antidepressants, including at least three distinct structural classes, showed substantial Na_V-channel block. Certain antidepressants, such as the tricyclic antidepressants amitriptyline[27,29] and imipramine[46], are known to block multiple Na_V channels in a use-dependent manner. In addition, it is well known that many antidepressants are useful for treating pain[47–49], and it is possible that some of this activity is related to Na_V-channel block. However, blockade of Na_V channels is not generally regarded as a common

feature among antidepressant drugs. In particular, Na_v-channel block has not been reported for the structurally distinct selective serotonin reuptake inhibitor antidepressants sertraline and paroxetine. Our data suggest that these drugs block Na_v channels in the 2–5 μM range, which is at the high end of therapeutic blood levels for sertraline and at least tenfold above those of paroxetine[20]. However, these drugs likely reach much higher concentrations in their target tissues as they enrich in rodent brains 24- and threefold relative to plasma, respectively[21]. It is likely, therefore, that at therapeutic doses, antidepressants achieve levels in the central nervous system sufficient to block Na_v channels. Our data would therefore suggest either that there is a high degree of structure-activity relationship overlap between antidepressant targets and Na_v blockers or that Na_v blockade contributes to the activity of antidepressants. The finding of this high correlation may spur further investigation into the role of Na_v blockade in the pharmacological action of this drug class.

Although the E-VIPR experiments presented here were focused on detecting and characterizing Na_v blockers using voltage dyes in recombinant cells, our approach is applicable to other ion-channel classes, modulator types, detection methods and cell systems. For example, it could be adapted to study voltage-gated Ca^{2+} channels using fluorescent Ca^{2+} indicators or to image heterogeneous populations of primary neurons. Thus, our approach should facilitate the exploration of voltage-gated channels and excitable cells for both basic research and drug discovery applications.

METHODS

Materials. Tetracaine, mexiletine, lidocaine, amitriptyline, pluronic F-127, TTX and β-cyclodextrin were obtained from Sigma. Approximately 400 drugs screened were purchased from the following companies: Aldrich, BIOMOL International, CalBiochem, ChemBridge, Fluka, Isotec, Sigma, Sigma-RBI, US Pharmacopeia, OnBio, Toronto Research Chemicals, Asinex, InterBioScreen, Lipomed and Sequoia Research Products. CC2-DMPE (chlorocoumarin-2-dimyristoyl phosphatidylethanolamine), DiSBAC6(3) (bis-(1,3-dihexyl-thiobarbituric acid) trimethine oxonol)[17] and Acid Yellow 17 (ESS AY-17) were produced at Vertex Pharmaceuticals. CC2-DMPE is also commercially available from Invitrogen. Lamotrigine was purchased from Sciencelab.com. Dulbecco's modified essential medium (4.5 g/l D-glucose), MEM nonessential amino acids, HEPES, sodium-pyruvate, lipofectamine and blasticidin were obtained from Invitrogen. Fetal bovine serum was obtained from Hyclone. External bath solution (140 mM NaCl, 4.5 mM KCl, 1 mM $MgCl_2$, 2 mM $CaCl_2$, 10 mM glucose, 10 mM HEPES-NaOH, pH 7.3 with NaOH) used in the assay was obtained from MediaTech. Growth Factor Reduced matrigel matrix was obtained from BD Science.

Human $Na_v1.3$ cloning, expression and cell culture. cDNA encoding $hNa_v1.3$ was cloned using RT-PCR from human spinal cord RNA. A Kozaks like sequence and *Xhol* site were added to the 5′ end and a *NotI* site to the 3′ end of the $hNa_v1.3$ cDNA. The $hNa_v1.3$ cDNA was subsequently cloned (5′ to 3′) into the *XhoI*/*NotI* sites of pLBCX (+) using the *XhoI*/*Not* I restrictions sites. Retroviral vectors were generated through three-plasmid cotransfection using Lipofectamine. Retroviral transduction was used to infect HEK293 cells. The infected HEK293 cells stably expressing $hNa_v1.3$ were grown at 37 °C using Dulbecco's modified essential medium supplemented with 10% FBS, 5 μg/ml blasticidin, 1 mM sodium-pyruvate and 10 mM HEPES and subdivided every 3 to 4 d. For electrophysiological experiments, cells were grown on small coverslips and used for recording after 1–2 d in culture. The cloned $hNa_v1.3$ showed similar TTX sensitivity (IC_{50} = 2.8 nM) and voltage dependence of activation ($V_{0.5}$ = −26.2 ± 2.3 mV, n = 3) and steady-state inactivation ($V_{0.5}$ = −60 ± 0.4 mV, n = 4) to the previous reported values[22].

E-VIPR assay preparation. Cells were cultured on 96-well plates (Costar tissue culture-treated 96-well flat bottom plates, Corning) precoated with 0.5% Growth Factor Reduced matrigel matrix in DMEM for 1 h at 23 °C. About 40,000 cells were added to each well and incubated at 37 °C for 24 h before being assayed at 23 °C. Test compounds were prepared from 10 mM DMSO stock solutions and prespotted into polypropylene plates before diluting to 2× with external bath solution containing 1 mM ESS AY17. The cell plates were first washed three times with external solution using an automatic plate washer (ELx405, Biotek), leaving a 50 μl/well residual volume. Subsequently, 50 μl/well of mixed dye solution of 10 μM CC2-DMPE, 2.4 μM $DiSBAC_6(3)$, 0.5% β-cyclodextrin and 20 μg/ml pluronic F-127 in external solution, was added to the cell plates. Following 30 min incubation in the dark at 23 °C, the cells were washed three times again with external solution, leaving a 50 μl/well residual volume. The final compound solutions were then added to the cell plates at 1:1 ratio to obtain desired final concentrations. Cells were incubated with test compounds for 30 min before being assayed.

Electrophysiology. Recordings were made at 23 °C using an Axopatch 200A amplifier and pClamp9 software (Axon Instruments). The same external solution used for the E-VIPR assay was used for whole-cell recordings. For voltage-clamp recording, the intracellular solution was 130 mM CsF, 10 mM NaCl, 1 mM $MgCl_2$, 10 mM HEPES (acids), 1.5 mM EGTA and 10 mM glucose, pH 7.3 with CsOH. For current-clamp recording, the intracellular solution was 150 mM KCl, 10 mM NaCl, 1 mM $MgCl_2$, 10 mM HEPES (acid), 1.5 mM EGTA and 10 mM glucose, pH 7.3 with KOH. The resistance of whole-cell patch pipettes fabricated from Kimax-51 glass capillaries (Fisher Scientific) was 1 to 2 MΩ when filled with Cs^+/Na^+ or K^+/Na^+ pipette solution. Data were digitally acquired by filtering at 10 kHz and sampling at 50 kHz. Data traces were subsequently filtered at 3 kHz for analysis and presentation. Capacitance transients were not subtracted. Leak currents were corrected with built-in function of the amplifier. For whole-cell recording, series resistance was electronically compensated to at least 70%. Only cells forming seal resistance > 2 GΩ were used for recordings, otherwise discarded. The cell line used has a resting membrane potential near −65 mV. The voltage-clamp protocol used to compare with E-VIPR included a step to −65 mV from a holding potential of −120 mV to match the resting potential. Current-clamp recordings (**Fig. 2b**) were recorded at 2 kHz and held at −75 mV before current injection.

E-VIPR: electrical field stimulation. Protocols, including waveform, timing, frequency and repetition of stimulations, were defined via a graphical user interface of a custom program running in MS Windows system. A custom-designed amplifier was used to generate the final voltage pulses. These voltage pulses were delivered with eight pairs of electrodes to simultaneously create an electrical field in a column of eight wells of a 96-well plate[18]. Each cell plate was sequentially stimulated from columns 1 to 12 using 2-ms monophasic voltage pulses stepping from 0 to 40 V, delivered at frequencies of 1, 5 and 10 Hz. As the distance between two electrodes was 0.4 cm, the resulting electrical field was up to 113 V/cm.

E-VIPR data acquisition and analysis. HEK293 cells stained with CC2-DMPE and $DiSBAC_6(3)$ were excited at 400 ± 7.5 nm. Fluorescence responses were collected at 460 ± 22.5 nm for CC2-DMPE and 580 ± 30 nm for $DiSBAC_6(3)$. The original emission fluorescence was analog low-pass filtered at 1 kHz, digitized at 5 kHz, and boxcar averaged down to 200 Hz before being stored to hard drive. The collected fluorescence signals were subtracted with the background fluorescence obtained in cell-free wells (column 12) of the same cell plate, and were normalized using the equation $\Delta F = F/F_o - 1$, where ΔF is the change of normalized fluorescence emission, F is fluorescence emission and F_o is the average baseline fluorescence emission before stimulation. Normalized CC2-DMPE over $DiSBAC_6(3)$ fluorescence emission ratio, or FRET ratio, was used to monitor changes in cellular membrane potential and calculated using the equation $\Delta R = R/R_o - 1$ where ΔR is the change of the normalized FRET ratio, R is the FRET ratio and R_o is the average ratio before stimulation. Measuring the FRET ratio maximizes the signal change and reduces experimental artifacts.

Analysis of compound activity. Test compound activity was determined from the amplitude of peak inward current or FRET ratio response elicited by the first (P1) and 20th (P20) stimulation pulses in the presence and absence of test compound. The block obtained at P1 and P20 was referred to baseline and use-dependent block, respectively. '% blocking activity' was defined as $(1 - \Delta R_F/\Delta R_{NB}) \times 100$, where ΔR_B and ΔR_{NB} denote the normalized peak ratio response

or peak inward current obtained in the presence and absence of blockers, respectively. Concentration-response curves were fit to (100 − %block activity) = [blocker]^n/([blocker]^n + $(IC_{50})^n$), carried out in SigmaPlot 2000 (SPSS) or Origin 7 (OriginLab). IC_{50} is the blocker's 50% inhibition concentration and n is the slope.

ACKNOWLEDGMENTS

We thank Charlie Cohen, Jennings Worley, Jeff Stack and Kevin Beaumont for review of manuscript and providing useful suggestions.

COMPETING INTERESTS STATEMENT

The authors declare that they have no competing financial interests.

1. Brau, M.E., Deimmann, M., Olschewski, A., Vogel, W. & Hempelmann, G. Effect of drugs used for neuropathic pain management on tetrodotoxin-resistant Na(+) currents in rat sensory neurons. *Anesthesiology* **94**, 137–144 (2001).
2. Carmeliet, E. & Mubagwa, K. Antiarrhythmic drugs and cardiac ion channels: mechanisms of action. *Prog. Biophys. Mol. Biol.* **70**, 1–72 (1998).
3. White, H.S. Comparative anticonvulsant and mechanistic profile of the established and newer antiepileptic drugs. *Epilepsia* **40** suppl. Suppl 5, 52–10 (1999).
4. Courtney, K.R. Mechanism of frequency-dependent inhibition of sodium currents in frog myelinated nerve by the lidocaine derivative GEA. *J. Pharmacol. Exp. Ther.* **195**, 225–236 (1975).
5. Scholz, A. Mechanisms of (local) anaesthetics on voltage-gated sodium and other ion channels. *Br. J. Anaesth.* **89**, 52–61 (2002).
6. Clare, J.J., Tate, S.N., Nobbs, M. & Romanos, M.A. Voltage-gated sodium channels as therapeutic targets. *Drug Discov. Today* **5**, 506–520 (2000).
7. Schroeder, K., Neagle, B., Trezise, D.J. & Worley, J. IonWorks HT: a new high-throughput electrophysiology measurement platform. *J. Biomol. Screen.* **8**, 50–64 (2003).
8. Wood, C., Williams, C. & Waldron, G.J. Patch clamping by numbers. *Drug Discov. Today* **9**, 434–441 (2004).
9. Bennett, P.B. & Guthrie, H.R. Trends in ion channel drug discovery: advances in screening technologies. *Trends Biotechnol.* **21**, 563–569 (2003).
10. Worley, J.F., III & Main, M.J. An industrial perspective on utilizing functional ion channel assays for high throughput screening. *Receptors Channels* **8**, 269–282 (2002).
11. Zheng, W., Spencer, R.H. & Kiss, L. High throughput assay technologies for ion channel drug discovery. *Assay Drug Dev. Technol.* **2**, 543–552 (2004).
12. Felix, J.P. *et al.* Functional assay of voltage-gated sodium channels using membrane potential-sensitive dyes. *Assay Drug Dev. Technol.* **2**, 260–268 (2004).
13. Maher, M.P. & Gonzalez, J.E. Multi-well plate and electrode assemblies for ion channel assays. US patent 6,969,449 B2 (2005).
14. Maher, M.P. & Gonzalez, J.E. High throughput method and system for screening candidate compounds for activity against ion channels. US patent 6,686,193 B2 (2004).
15. Kim, C.H., Oh, Y., Chung, J.M. & Chung, K. The changes in expression of three subtypes of TTX sensitive sodium channels in sensory neurons after spinal nerve ligation. *Brain Res. Mol. Brain Res.* **95**, 153–161 (2001).
16. Black, J.A., Liu, S., Tanaka, M., Cummins, T.R. & Waxman, S.G. Changes in the expression of tetrodotoxin-sensitive sodium channels within dorsal root ganglia neurons in inflammatory pain. *Pain* **108**, 237–247 (2004).
17. Gonzalez, J.E. & Tsien, R.Y. Voltage sensing by fluorescence resonance energy transfer in single cells. *Biophys. J.* **69**, 1272–1280 (1995).
18. Gonzalez, J.E. & Tsien, R.Y. Improved indicators of cell membrane potential that use fluorescence resonance energy transfer. *Chem. Biol.* **4**, 269–277 (1997).
19. Gonzalez, J.E., Oades, K., Leychkis, Y., Harootunian, A. & Negulescu, P.A. Cell-based assays and instrumentation for screening ion-channel targets. *Drug Discov. Today* **4**, 431–439 (1999).
20. Mao, J. & Chen, L.L. Systemic lidocaine for neuropathic pain relief. *Pain* **87**, 7–17 (2000).
21. Lenkowski, P.W., Shah, B.S., Dinn, A.E., Lee, K. & Patel, M.K. Lidocaine block of neonatal Nav1.3 is differentially modulated by co-expression of beta1 and beta3 subunits. *Eur. J. Pharmacol.* **467**, 23–30 (2003).
22. Postma, S.W. & Catterall, W.A. Inhibition of binding of 125I-labeled α-scorpion toxin to sodium channels by local anesthetics. *Mol. Pharmacol.* **25**, 219–227 (1984).
23. Conti, F., Gheri, A., Pusch, M. & Moran, O. Use dependence of tetrodotoxin block of sodium channels: a revival of the trapped-ion mechanism. *Biophys. J.* **71**, 1295–1312 (1996).
24. Eickhorn, R., Weirich, J., Hornung, D. & Antoni, H. Use dependence of sodium current inhibition by tetrodotoxin in rat cardiac muscle: influence of channel state. *Pflugers Arch.* **416**, 398–405 (1990).
25. John, V.H. *et al.* Heterologous expression and functional analysis of rat NaV1.8 (SNS) voltage-gated sodium channels in the dorsal root ganglion neuroblastoma cell line ND7-23. *Neuropharmacology* **46**, 425–438 (2004).
26. Song, J.H., Huang, C.S., Nagata, K., Yeh, J.Z. & Narahashi, T. Differential action of riluzole on tetrodotoxin-sensitive and tetrodotoxin-resistant sodium channels. *J. Pharmacol. Exp. Ther.* **282**, 707–714 (1997).
27. Wang, G.K., Russell, C. & Wang, S.Y. State-dependent block of voltage-gated Na+ channels by amitriptyline via the local anesthetic receptor and its implication for neuropathic pain. *Pain* **110**, 166–174 (2004).
28. Nau, C., Seaver, M., Wang, S.Y. & Wang, G.K. Block of human heart hH1 sodium channels by amitriptyline. *J. Pharmacol. Exp. Ther.* **292**, 1015–1023 (2000).
29. Bielefeldt, K., Ozaki, N., Whitlon, C. & Gebhart, G.F. Amitriptyline inhibits voltage-sensitive sodium currents in rat gastric sensory neurons. *Dig. Dis. Sci.* **47**, 959–966 (2002).
30. Ragsdale, D.S., McPhee, J.C., Scheuer, T. & Catterall, W.A. Molecular determinants of state-dependent block of Na+ channels by local anesthetics. *Science* **265**, 1724–1728 (1994).
31. Akiba, I. *et al.* Stable expression and characterization of human PN1 and PN3 sodium channels. *Receptors Channels* **9**, 291–299 (2003).
32. Kuo, C.C. & Lu, L. Characterization of lamotrigine inhibition of Na+ channels in rat hippocampal neurones. *Br. J. Pharmacol.* **121**, 1231–1238 (1997).
33. Lang, D.G., Wang, C.M. & Cooper, B.R. Lamotrigine, phenytoin and carbamazepine interactions on the sodium current present in N4TG1 mouse neuroblastoma cells. *J. Pharmacol. Exp. Ther.* **266**, 829–835 (1993).
34. Xie, X., Lancaster, B., Peakman, T. & Garbinwale, J. Interaction of the antiepileptic drug lamotrigine with recombinant rat brain type IIA Na+ channels and with native Na+ channels in rat hippocampal neurones. *Pflugers Arch.* **430**, 437–446 (1995).
35. Hebert, T., Drapeau, P., Pradier, L. & Dunn, R.J. Block of the rat brain IIA sodium channel alpha subunit by the neuroprotective drug riluzole. *Mol. Pharmacol.* **45**, 1056–1060 (1994).
36. Zhang, J.H., Chung, T.D. & Oldenburg, K.R. A Simple statistical parameter for use in evaluation and validation of high throughput screening assays. *J. Biomol. Screen.* **4**, 67–73 (1999).
37. Fera, M. *The Ambiguous Frog: The Galvani-Volta Controversy on Animal Electricity* (Princeton University Press, Princeton, N.J., 1992).
38. Basser, P.J. & Roth, B.J. New currents in electrical stimulation of excitable tissues. *Annu. Rev. Biomed. Eng.* **2**, 377–397 (2000).
39. Roth, B.J. Mechanisms for electrical stimulation of excitable tissue. *Crit. Rev. Biomed. Eng.* **22**, 253–305 (1994).
40. Benabid, A.L. *et al.* Therapeutic electrical stimulation of the central nervous system. *C. R. Biol.* **328**, 177–186 (2005).
41. Burnett, P. *et al.* Fluorescence imaging of electrically stimulated cells. *J. Biomol. Screen.* **8**, 660–667 (2003).
42. Baxter, D.F. *et al.* A novel membrane potential-sensitive fluorescent dye improves cell-based assays for ion channels. *J. Biomol. Screen.* **7**, 79–85 (2002).
43. Leffler, A., Herzog, R.I., Dib-Hajj, S.D., Waxman, S.G. & Cummins, T.R. Pharmacological properties of neuronal TTX-resistant sodium channels and the role of a critical serine pore residue. *Pflugers Arch.* **451**, 454–463 (2005).
44. Tomiak, S.A., Rosenberg, R.L., Emerick, M.C. & Agnew, W.S. Fluorescence assay for neurotoxin-modulated ion transport by the reconstituted voltage-activated sodium channel isolated from eel electric organ. *Biochemistry* **25**, 2162–2174 (1986).
45. Vickery, R.G. *et al.* Comparison of the pharmacological properties of rat NaV1.8 with rat NaV1.2a and human NaV1.5 voltage-gated sodium channel subtypes using a membrane potential sensitive dye and FLIPR. *Receptors Channels* **10**, 11–23 (2004).
46. Yang, Y.C. & Kuo, C.C. Inhibition of Na(+) current by imipramine and related compounds: different binding kinetics as an inactivation stabilizer and as an open channel blocker. *Mol. Pharmacol.* **62**, 1228–1237 (2002).
47. Abdi, S., Lee, D.H. & Chung, J.M. The anti-allodynic effects of amitriptyline, gabapentin, and lidocaine in a rat model of neuropathic pain. *Anesth. Analg.* **87**, 1360–1366 (1998).
48. Carter, G.T. & Sullivan, M.D. Antidepressants in pain management. *Curr. Opin. Investig. Drugs* **3**, 454–458 (2002).
49. Mazels, M. & McCarberg, B. Antidepressants and antiepileptic drugs for chronic non-cancer pain. *Am. Fam. Physician* **71**, 483–490 (2005).
50. Schulz, M. & Schmoldt, A. Therapeutic and toxic blood concentrations of more than 800 drugs and other xenobiotics. *Pharmazie* **58**, 447–474 (2003).
51. Doran, A. *et al.* The impact of P-glycoprotein on the disposition of drugs targeted for indications of the central nervous system: evaluation using the MDR1A/1B knockout mouse model. *Drug Metab. Dispos.* **33**, 165–174 (2005).
52. Chen, Y.H. *et al.* Cloning, distribution and functional analysis of the type III sodium channel from human brain. *Eur. J. Neurosci.* **12**, 4281–4289 (2000).